

---

**ELECTRONIC AND OPTICAL PROPERTIES  
OF SEMICONDUCTORS**

---

# Mechanisms of Recombination of Nonequilibrium Charge Carriers in Epitaxial $\text{Cd}_x\text{Hg}_{1-x}\text{Te}$ ( $x = 0.20\text{--}0.23$ ) Layers

D. G. Ikusov<sup>a</sup>, F. F. Sizov<sup>b</sup>, S. V. Staryi<sup>b</sup>, and V. V. Teterkin<sup>b</sup>

<sup>a</sup>*Institute of Semiconductor Physics, Siberian Division, Russian Academy of Sciences, Novosibirsk, 630090 Russia*

<sup>b</sup>*Lashkarev Institute of Semiconductor Physics, National Academy of Sciences of Ukraine, Kiev, 03025 Ukraine*

<sup>^</sup>*e-mail: ssv1811@i.com.ua*

Submitted February 3, 2006; accepted for publication April 7, 2006

**Abstract**—The experimental temperature dependences of the photosensitivity and the data on the lifetime of nonequilibrium charge carriers in epitaxial  $\text{Cd}_x\text{Hg}_{1-x}\text{Te}$  layers with  $x = 0.20\text{--}0.23$  were used to show that, in the region of intrinsic and extrinsic conductivity in  $n$ -type films grown by molecular beam epitaxy, CHCC Auger recombination is the prevailing recombination mechanism. At the same time, in  $p$ -type films grown by liquid- or vapor-phase epitaxy, it is observed that, in the region of extrinsic conductivity, CHLH Auger recombination competes with Shockley–Read recombination. The  $n$ -type films grown by molecular beam epitaxy contain a much lower concentration of recombination centers than the  $p$ -type films grown by liquid- or gas-phase epitaxy.

PACS numbers: 72.40.+w, 73.50.Cr

DOI: 10.1134/S1063782607020029

## 1. INTRODUCTION

It is known that the characteristics of semiconductor photodiodes depend on the main parameter of the semiconductor material, i.e., the lifetime of nonequilibrium charge carriers [1, 2]. The lifetime, in turn, is defined by the recombination mechanism prevailing in a particular temperature region. The competition between different recombination mechanisms is especially well-pronounced in the narrow-gap semiconductors, specifically in the  $\text{Cd}_x\text{Hg}_{1-x}\text{Te}$  (MCT) compounds. Because of the narrow band gap and large ratio between the effective masses of heavy holes and electrons in these semiconductors, interband mechanisms, i.e., Auger recombination and radiative recombination, are of considerable importance, along with extrinsic Shockley–Read recombination. The interband recombination is characteristic of the intrinsic material and cannot be eliminated in principle, whereas Shockley–Read recombination is controlled by impurities and defects, i.e., by the degree of technological sophistication of the production process. It is known that the extrinsic recombination defines to a large extent the mechanisms of charge transport and the threshold parameters of diodes fabricated by implantation or diffusion on the basis of epitaxial  $n$ - or  $p$ -type  $\text{Cd}_x\text{Hg}_{1-x}\text{Te}$  films [2].

At the present time, the origin of the Shockley–Read recombination centers in epitaxial  $\text{Cd}_x\text{Hg}_{1-x}\text{Te}$ -based films and diodes is unknown. Because the available data on the recombination mechanisms in epitaxial MCT films are contradictory, this issue remains open.

The goal of this study was to investigate the lifetime of nonequilibrium charge carriers in epitaxial MCT films grown by different technological procedures in order to establish the prevailing recombination mechanisms.

## 2. EXPERIMENTAL

We studied the temperature dependences of the lifetime of nonequilibrium charge carriers in the epitaxial  $\text{Cd}_x\text{Hg}_{1-x}\text{Te}$  ( $x = 0.20\text{--}0.23$ ) films produced by molecular beam epitaxy (MBE), vapor-phase epitaxy (VPE), and liquid-phase epitaxy (LPE). The studies were carried out at temperatures  $T$  ranging from 77 to 300 K. The nonequilibrium charge carriers were excited by a pulsed GaAs laser beam at the wavelength  $\lambda = 0.88\ \mu\text{m}$ . The laser radiation intensity corresponded to the condition of low excitation levels. The lifetime  $\tau$  was determined from the decay of the unsteady-photoconductivity signal recorded by a S1-70 wide-band oscilloscope. We examined more than 20 epitaxial film samples grown by the above-listed procedures. The parameters (the concentration of electrons  $n$  and holes  $p$  and the mobility  $\mu$  of charge carriers) of the typical samples produced by each of the above-mentioned technological procedures are listed in the table.

The  $n$ -type films were grown by MBE at a temperature of 190°C. The substrates were GaAs single-crystal wafers on which we successively deposited ZnTe and CdTe buffer layers with the thickness of about 0.3 and 6  $\mu\text{m}$ , respectively. To suppress recombination at the film surface and at the film–substrate interface, we

Typical parameters of epitaxial film samples fabricated by different procedures

Sample no.	Conductivity type	Technology	$x$	$n, p, \text{cm}^{-3}$	$\mu, \text{cm}^2 \text{V}^{-1} \text{s}^{-1}$	$\tau, \text{ns} (T = 77 \text{ K})$
1	$n$	MBE	0.22	$1.2 \times 10^{15}$	$6.8 \times 10^4$	$10^3$
2	$p$	VPE	0.23	$2.3 \times 10^{16}$	380	10
3	$p$	LPE	0.2	$2.45 \times 10^{16}$	400	15

grew graded-gap layers with the suitable variation in composition over the thickness. Specifically, the composition at the film surface corresponded to  $x \approx 0.3$ . The thickness of the central part of the film with  $x = 0.22$  was 10–15  $\mu\text{m}$ .

The  $p$ -type epitaxial MCT layer samples were grown by VPE and LPE. The VPE epitaxial layers were grown using isothermal evaporation (at 600°C) followed by diffusion of the Hg atoms from the HgTe source onto the CdTe substrate placed at a small (5 mm) distance from the source. The distribution of the composition of the film over the thickness was monitored by secondary-ion mass spectroscopy. The surface layer with a high compositional gradient over the thickness was removed by chemical etching. The layers homogeneous in composition were no thinner than 20  $\mu\text{m}$ . At  $T = 77 \text{ K}$ , the concentration of holes in the layers was  $p = (2\text{--}8) \times 10^{16} \text{ cm}^{-3}$ . The LPE layers were grown from a solution enriched with tellurium on the CdZnTe substrate at the temperature of 500°C and the pressure of the Hg vapors  $\sim 0.1 \text{ atm}$ . The samples produced under these conditions were of the  $p$  type; the concentration of charge carriers was  $5 \times 10^{15}\text{--}6 \times 10^{16} \text{ cm}^{-3}$ . In the films,

the thickness of the layer homogeneous in composition was 10–16  $\mu\text{m}$ . The typical dependences of the photosensitivity of the  $n$ - and  $p$ -type films are shown in Fig. 1. The temperature dependences of the lifetime are shown in Figs. 2 and 3.

### 3. DISCUSSION

The photosensitivity of the  $n$ -type samples decreases with increasing temperature. At the same time, an increase in the photosensitivity is, as a rule, observed for the  $p$ -type samples as temperature increases (Fig. 1). If the photoconductivity is measured under short-circuit conditions (when the load resistance is much lower than the resistance of the sample), the value of the photoresponse signal can be found from the relation [3]

$$U_{\text{ph}} = e\Delta n(\mu_n + \mu_p)UR,$$

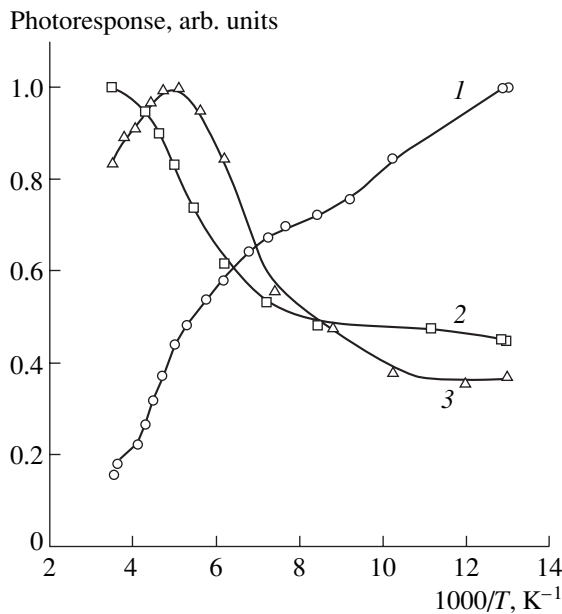


**Fig. 1.** Temperature dependences of the photosensitivity of the (1)  $n$ - and (2, 3)  $p$ -type  $\text{Cd}_x\text{Hg}_{1-x}\text{Te}$  films grown by (2) VPE and (3) LPE.

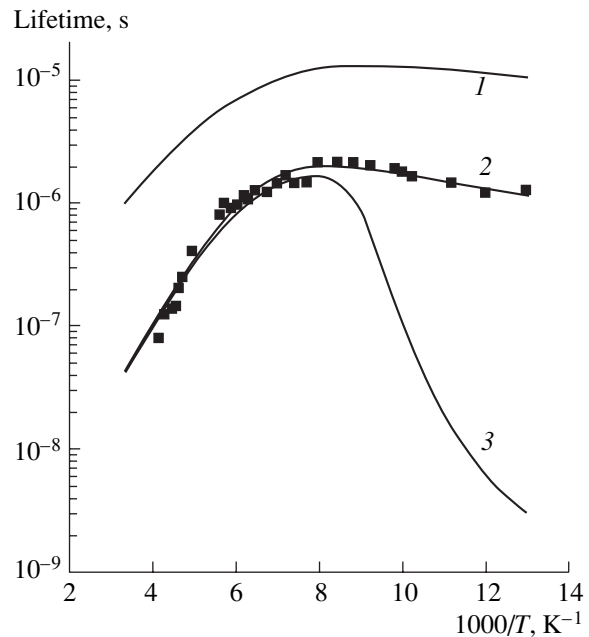


**Fig. 2.** Temperature dependences of the lifetime in the epitaxial  $n\text{-Cd}_x\text{Hg}_{1-x}\text{Te}$  film (sample 1). The solid squares refer to the experimental data; the solid lines refer to the results of calculations of the lifetimes with respect to (1) radiative recombination and (2) CHCC Auger recombination. Curve 3 shows the resulting dependence calculated with regard to recombination via impurities at the concentration of recombination centers  $N_T = 1.3 \times 10^{14} \text{ cm}^{-3}$ .

where  $\Delta n$  is the concentration of nonequilibrium charge carriers,  $U$  is the supply voltage,  $R$  is the load resistance, and  $\mu_n$  and  $\mu_p$  are the mobilities of electrons and holes, with  $\mu_n \gg \mu_p$ . If we take into account that the pulse duration is  $\tau_p < \tau$  and the lifetime varies only slightly in the temperature region under study, we may assume that, with the slight temperature dependence of  $\Delta n$  disregarded, the temperature dependence of the photoresponse signal is bound to follow the temperature dependence of the charge carrier mobility, or more exactly, of the sum of the mobilities of the majority and minority charge carriers. In the low-temperature region, scattering of charge carriers by impurities and intrinsic lattice defects prevails; therefore, with elevating temperature, the charge-carrier mobility increases proportionally to  $T^{3/2}$ . In the high-temperature region, scattering at thermal lattice vibrations, i.e., phonons, plays a dominant role, and therefore, the mobility decreases as  $T^{-3/2}$  (or follows a power-law dependence with a negative exponent that can be even larger in magnitude than  $3/2$ , even reaching  $-3$ ). Thus, the temperature dependence of the mobility is expected to show a maximum at the point at which the contributions of both mechanisms of scattering are comparable. The temperature position of the maximum is expected to depend on the quality of the material. In fact, a shift of the maximum of the photosensitivity to higher temperatures suggests that there is a higher concentration of impurities and extrinsic defects in the material.

From Fig. 1 it can be seen that, for the  $n$ -type samples (curve 1), the maximum should be at low temperatures (below 77 K), suggesting that the epitaxial layers grown by MBE are of high quality and high purity (similar curves were presented in [4]). For the  $p$ -type samples grown by VPE and LPE, the maximum is either observed at high temperatures beyond the region under consideration (curve 2) or shifted to temperatures somewhat below room temperature (curve 3), suggesting that the films are of lower quality. It follows from the slope of the curves of the photosensitivity in the low-temperature region for different  $p$ -type samples that the temperature dependence is between  $\propto T^{0.5}$  and  $\propto T^{1.3}$ . At the same time, in the high-temperature region, the slope of the curves corresponding to the dependence  $\propto T^{-2.9}$  may suggest that, as noted in [5], there are mechanical strains of compression or extension typical of epitaxial films.

The contribution of various recombination mechanisms to the charge-carrier lifetime in the  $\text{Cd}_x\text{Hg}_{1-x}\text{Te}$  single crystals with  $x = 0.20\text{--}0.23$  was analyzed in a number of studies [6–11]. It was shown that, in the  $n$ - and  $p$ -type materials, the prevailing recombination mechanism at high temperatures is Auger recombination [6]. In this case, for the  $n$ -type MCT materials, the CHCC process is essential. The CHCC process implies recombination of an electron with a free hole, with the energy transfer to another free electron. In  $p$ -type materials, the CHLH process plays a major part. In this

process, the energy released on recombination is spent for the transition of an electron from the band of light holes to the band of heavy holes.

We calculated the temperature dependences of the lifetime of nonequilibrium charge carriers in cases of different recombination mechanisms in  $n$ - and  $p$ -type  $\text{Cd}_x\text{Hg}_{1-x}\text{Te}$  materials at low-intensity excitation levels, i.e., at  $\Delta n = \Delta p \ll n_0, p_0$  ( $\Delta n$  and  $\Delta p$  are the concentrations of nonequilibrium and equilibrium electrons and holes, respectively, and  $n_0$  and  $p_0$  are the concentrations of equilibrium electrons and holes). For  $n$ -type MCT materials, the Auger recombination rates were determined from the relations for the lifetime with respect to the electron–electron (CHCC) process [7],

$$\tau_{A1} = \frac{2\tau_{A1}^i}{1 + (n_0/n_i)^2}, \quad (1)$$

where  $n_i$  is the intrinsic concentration of charge carriers and  $\tau_{A1}^i$  is the intrinsic lifetime with respect to the CHCC process, as defined in [7]. In the calculations, the value of the overlap integral for the wave functions was taken to be  $|F_1F_2| = 0.3$ .

The lifetime with respect to the CHLH processes can be found from the relations [8]

$$\tau_A = \frac{2\gamma\tau_{A1}^i}{1 + \gamma + \gamma(n_0/n_i)^2 + (p_0/n_i)^2}, \quad (2)$$

$$\gamma = \frac{\tau_{A7}^i}{\tau_{A1}^i} \approx 6 \left(1 - \frac{5E_g}{4kT}\right) \left(1 - \frac{3E_g}{2kT}\right)^{-1}, \quad (3)$$

where  $\tau_{A7}^i$  is the intrinsic lifetime with respect to the CHLH process,  $E_g$  is the band gap, and  $k$  is the Boltzmann constant.

According to the calculations for the pure MCT materials with  $x = 0.22$  and  $n = 5 \times 10^{14} \text{ cm}^{-3}$ , the lifetime with respect to the CHCC process is  $\sim 6.3 \times 10^{-6} \text{ s}$  at 77 K. For the  $p$ -type films of the same composition, with the concentration of holes of  $\sim 10^{16} \text{ cm}^{-3}$ , the lifetime with respect to the CHLH process is  $8 \times 10^{-8} \text{ s}$ .

The lifetime with respect to radiative recombination was calculated according to van Roosbroeck–Shockley's theory [9]:

$$\tau_R = \frac{2\tau_R^i}{1 + n_0/n_i}. \quad (4)$$

Here,  $\tau_R^i$  is the intrinsic lifetime with respect to the radiative recombination mechanism. The quantity  $\tau_R^i$  is defined in terms of the radiative recombination coefficient  $G_R$  as

$$\tau_R^i = \frac{n_i}{2G_R}. \quad (5)$$

The expression for  $G_R$  is given, e.g., in [9]. For the MCT films with  $x = 0.22$  and  $n = 5 \times 10^{14} \text{ cm}^{-3}$  at the liquid-nitrogen temperature, the calculated lifetime with respect to the radiative process is  $\sim 2.4 \times 10^{-5} \text{ s}$ . For the  $p$ -type films of the same composition, with  $p = 10^{16} \text{ cm}^{-3}$ , this lifetime is equal to  $1.2 \times 10^{-6} \text{ s}$ , which is an order of magnitude longer than the lifetime with respect to the Auger recombination. This relation between the lifetimes with respect to these recombination mechanisms is valid at other temperatures too, specifically, up to room temperature and higher. Consequently, the radiative process does not play any noticeable part in the MCT film of this composition.

The contribution of the Shockley–Read recombination via impurities increases with decreasing temperature. In this case, the purer the MCT material, the lower the temperature at which the impurity recombination begins to prevail. For example, in the high-purity  $n\text{-Cd}_x\text{Hg}_{1-x}\text{Te}$  with  $x = 0.2$  ( $\mu_n = (2\text{--}2.5) \times 10^5 \text{ cm}^2/(\text{V s})$ ) at the liquid-nitrogen temperature, the CHCC mechanism prevails [6] and the lifetime is 2–3  $\mu\text{s}$ . For not so pure compensated crystals with the mobility  $\mu < 10^5 \text{ cm}^2/(\text{V s})$  at 77 K, Shockley–Read recombination via a series of acceptor centers prevails [6]; the corresponding acceptor levels are 10–70 meV above the top of the valence band [6]. In pure uncompensated  $p\text{-Cd}_x\text{Hg}_{1-x}\text{Te}$  crystals (with  $x = 0.2$ ) in which the concentration of uncompensated acceptors is  $N_A - N_D \approx 10^{15}\text{--}10^{16} \text{ m}^{-3}$ , recombination via impurities prevails; in this case, the recombination occurs via two groups of recombination levels at 10–15 and 30–50 meV from the top of the valence band.

There are some reported data in favor of the fact that the centers associated with the mercury vacancies produce levels in the band gap at the energies  $E_t = 0.75E_g$  and  $E_t = 0.37E_g$  above the top of the valence band [10, 12]. The deeper level is more important from the standpoint of being involved in recombination via impurities. The available data on the concentration of recombination centers,  $N_t$ , differ by more than two orders of magnitude, varying from  $1.3 \times 10^{14} \text{ cm}^{-3}$  [11] to  $4.3 \times 10^{16} \text{ cm}^{-3}$  [13]. In calculating the lifetime, the energy of the level was taken to be  $E_t = 0.37E_g$  and the values of  $N_t$  to be within the above-indicated range.

At low excitation levels and low concentrations of recombination centers, the lifetimes of the majority and minority charge carriers are

$$\tau_{SR} = \frac{\tau_{p0}(n_0 + n_1) + \tau_{n0}(p_0 + p_1)}{n_0 + p_0}. \quad (6)$$

At the same time, at high concentrations of recombination centers, it is necessary to determine the lifetimes of electrons and holes separately:

$$\tau_{SR}^p = \frac{\tau_{n0}(p_0 + p_1) + \tau_{p0}[n_0 + n_1 + N_t(1 + n_0/n_1)^{-1}]}{n_0 + p_0 + N_t(1 + n_0/n_1)^{-1}(1 + n_1/n_0)^{-1}}, \quad (7)$$

$$\tau_{SR}^n = \frac{\tau_{p0}(n_0 + n_1) + \tau_{n0}[p_0 + p_1 + N_t(1 + p_0/p_1)^{-1}]}{n_0 + p_0 + N_t(1 + p_0/p_1)^{-1}(1 + p_1/p_0)^{-1}}. \quad (8)$$

Here,  $n_1$  and  $p_1$  are the concentrations of electrons and holes in the corresponding bands with the Fermi level coinciding with the level of the recombination center, the parameters  $\tau_{n0}$  and  $\tau_{p0}$  are the minimal lifetimes of electrons and holes with respect to recombination via impurities,

$$\tau_{n0} = \frac{1}{\sigma_n V_{th} N_t} = \frac{1}{\gamma_n N_t}, \quad \tau_{p0} = \frac{1}{\sigma_p V_{th} N_t} = \frac{1}{\gamma_p N_t}, \quad (9)$$

$\sigma_n$  and  $\sigma_p$  are the capture cross-sections of the recombination centers for electrons and holes,  $V_{th}$  is the thermal velocity of charge carriers, and  $\gamma_n$  and  $\gamma_p$  are the Shockley–Read capture coefficients for electrons and holes. In general, the coefficients  $\gamma_n$  and  $\gamma_p$  are temperature-dependent and can be described by the empirical formulas [13]

$$\gamma_n(T) = \gamma_{n0} \left[ \frac{T}{77} \right]^{-\beta_n}, \quad \gamma_p(T) = \gamma_{p0} \left[ \frac{T}{77} \right]^{-\beta_p}. \quad (10)$$

The resulting lifetime with respect to recombination via impurities is commonly determined with regard to the different mobilities  $\mu_n$  and  $\mu_p$  for electrons and holes:

$$\tau_{SR} = \frac{\mu_n \tau_{SR}^n + \mu_p \tau_{SR}^p}{\mu_n + \mu_p}. \quad (11)$$

According to the calculation for the  $n\text{-Cd}_x\text{Hg}_{1-x}\text{Te}$  crystal with  $x = 0.22$ ,  $n = 5 \times 10^{14} \text{ cm}^{-3}$ , and the concentration of recombination centers  $N_t = 1.3 \times 10^{14} \text{ cm}^{-3}$ , the lifetime with respect to recombination via impurities is  $5 \times 10^{-8} \text{ s}$ . At the high concentration of recombination centers,  $N_t = 4.3 \times 10^{16} \text{ cm}^{-3}$ , the lifetime is  $4.1 \times 10^{-9} \text{ s}$ . For the  $p\text{-Cd}_x\text{Hg}_{1-x}\text{Te}$  crystal with  $x = 0.22$  and  $p = 10^{16} \text{ cm}^{-3}$ , the lifetimes with respect to recombination via impurities are, correspondingly,  $3 \times 10^{-7}$  and  $1.7 \times 10^{-9} \text{ s}$ .

The total, or so-called effective lifetime of charge carriers,  $\tau_{\text{eff}}$ , is determined by the relation

$$\frac{1}{\tau_{\text{eff}}} = \frac{1}{\tau_R} + \frac{1}{\tau_A} + \frac{1}{\tau_{SR}}. \quad (12)$$

Consequently, the value of  $\tau_{\text{eff}}$  is closer to the shortest lifetime among the lifetimes with respect to different recombination mechanisms.

The typical temperature dependence of the lifetimes in the  $n$ -type samples is shown in Fig. 2 (sample 1). In Fig. 2, the squares refer to the experimental data, and solid lines represent the results of theoretical calculations by formulas (1)–(5) for the lifetimes with respect to the basic channels of interband recombination, i.e., radiative recombination (curve 1) and CHCC Auger

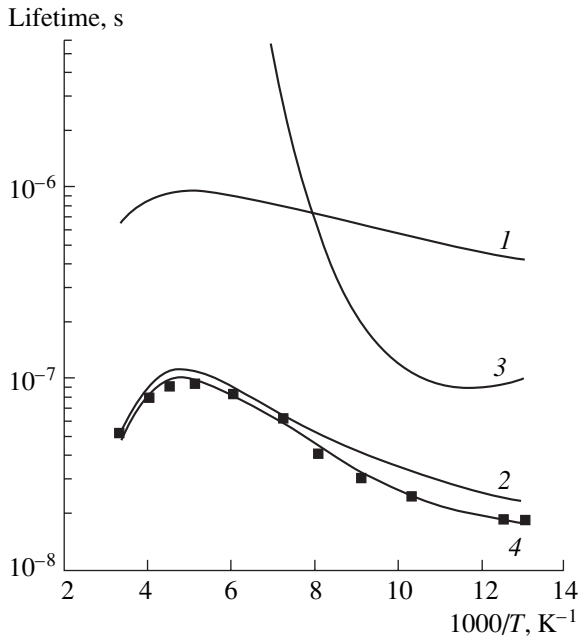


**Fig. 3.** Temperature dependences of the lifetime in the epitaxial  $p\text{-Cd}_x\text{Hg}_{1-x}\text{Te}$  film fabricated by VPE (sample 2). The solid squares refer to the experimental data. The solid lines refer to the results of calculations of the lifetimes with respect to (1) radiative recombination, (2) the CHCC and CHLH Auger recombination, and (3) Shockley–Read recombination via impurities at the concentration of recombination centers  $N_t = 3 \times 10^{15} \text{ cm}^{-3}$ . Curve 4 shows the resulting dependence calculated with regard to recombination via impurities.

recombination (curve 2); curve 3 corresponds to the total lifetime calculated by formula (12) with regard to Shockley–Read recombination via impurities (see formulas (6)–(11)). In calculating the lifetime with respect to the last-mentioned recombination channel, for the cross sections of the traps of charge carriers, we used the values given in [13]. These are as follows (see formula (9)):  $\gamma_{n0} = 3.2 \times 10^{-7} \text{ cm}^3/\text{s}$ ,  $\beta_n = 1$ ,  $\gamma_{p0} = 9.8 \times 10^{-7} \text{ cm}^3/\text{s}$ , and  $\beta_p = 0.3$ . The concentration of recombination centers was set at  $N_t = 1.3 \times 10^{14} \text{ cm}^{-3}$ . The fact that, in the low-temperature region, there is no noticeable effect of recombination via impurities is indicative of the low concentration of the centers,  $N_t \leq 10^{12}\text{--}10^{13} \text{ cm}^{-3}$ .

By measuring the photoconductivity of the films of this type, it is established that the photoresponse pulse consists of two exponential components, a fast component and a slow component (Fig. 2 shows the temperature dependence of the lifetime corresponding to the slow component). It can be assumed that the fast component is due to surface recombination. In this case, we can use the well-known relation [14] to estimate the surface recombination rate as  $s = d/2\tau_s$ , where  $d$  is the film thickness and  $\tau_s$  is the corresponding lifetime. Since the fast component is limited by the laser pulse duration and exhibits the characteristic time  $<50 \text{ ns}$ , we

consequently obtain  $s > 1.3 \times 10^4 \text{ cm/s}$ , which is by more than an order of magnitude larger than the known values of  $s$  reported previously for the epitaxial MCT films. For example, for the  $p\text{-Cd}_x\text{Hg}_{1-x}\text{Te}$  bulk crystals treated in a bromine–methanol etchant, the surface recombination rate is  $s \leq 630 \text{ cm/s}$  [15]. For the epitaxial films grown by LPE, it is found that the recombination rate is  $s \leq 10^3 \text{ cm/s}$  [16]. It is worth noting that the lifetime remains unchanged upon illumination of both sides of the sample, i.e., the side of the film and the side of the substrate. If the surface effect were well pronounced, a difference would be observed. Thus, we conclude that the fast component is due neither to surface recombination nor to recombination at the film–substrate interface.

At the same time, the fact that the fast component disappears first with increasing laser excitation intensity suggests that there exists a fast recombination channel that makes its contribution to the lifetime only at rather high concentrations of nonequilibrium charge carriers. This channel may be recombination via impurities, such that it makes itself clearly evident from the rather high concentrations  $\Delta n$  and, as obvious from Fig. 2, results in considerably shorter lifetimes, compared to the lifetimes controlled by the Auger recombination.

In the  $p$ -type samples produced by LPE and VPE, the temperature dependences of the lifetime were similar both qualitatively and quantitatively. Figure 3 shows the experimental dependence typical of these samples, together with the results of theoretical calculations. In the  $p$ -type samples studied here, the CHCC Auger recombination is the unambiguously prevailing recombination mechanism in the high-temperature region. At  $T < 140 \text{ K}$ , along with this mechanism, recombination via impurities becomes noticeable and, thus, competes with the Auger process down to the liquid-nitrogen temperature. From the experimental temperature dependences of the lifetime, it is possible to estimate some parameters of recombination via impurities in the samples. For example, in sample 2, the concentration of recombination centers is high:  $N_t = 3 \times 10^{15} \text{ cm}^{-3}$ . The parameters of the cross section of capture of an electron by the recombination center (see formula (9)) at the liquid-nitrogen temperature are  $\gamma_{n0} = 3 \times 10^{-7} \text{ cm}^3/\text{s}$  and  $\beta_n = 0.4$ ; it follows then that the trapping cross section is  $\sigma_n = 4.4 \times 10^{-15} \text{ cm}^2$ .

From the comparison of the lifetimes in the  $n$ - and  $p$ -type samples, we can conclude that there exist some regular trends. In the  $n$ -type films at  $T = 77 \text{ K}$ , the lifetime of nonequilibrium charge carriers is in the range from  $10^{-7}$  to  $10^{-6} \text{ s}$ . In the  $p$ -type samples, the typical lifetime is in the range from  $10^{-8}$  to  $10^{-7} \text{ s}$ . The lifetimes in the  $n$ -type samples are longer, since there is no contribution of recombination via impurities. At the same time, as follows from the calculations, the lifetime  $\tau$  in the  $p$ -type samples is shorter, because the CHLH Auger process and recombination via impurities make approximately identical contributions to the total lifetime.

The origin of recombination centers in the  $\text{Cd}_x\text{Hg}_{1-x}\text{Te}$  epitaxial layers and single crystals has not been unambiguously established. However, in a number of studies, it was found that the concentration of deep levels correlated with the concentration of holes; the latter is known to correlate with the content of the Hg vacancies in the  $\text{Cd}_x\text{Hg}_{1-x}\text{Te}$  compound. In this context, it was assumed that the Hg vacancy can introduce two states, a shallow state and a deep state, or the Hg vacancy can be involved in a more complex defect. In [12] it was shown that, in the nominally undoped  $\text{Cd}_x\text{Hg}_{1-x}\text{Te}$  compound, the concentration of deep traps,  $N_t$ , varies in the range from  $0.1N_A$  to  $10N_A$ , where  $N_A$  is the concentration of shallow acceptors. If it is assumed that in the  $p$ -type material, the concentration of holes is  $p \approx N_A$  and the lifetime is  $\sim 10^{-7}$  s, typical of nonequilibrium charge carriers, the trapping cross section  $\sigma_n$  is in the range from  $10^{-15}$  to  $10^{-17}$   $\text{cm}^2$ . It can be assumed that a decrease in the concentration of Hg vacancies is accompanied by a decrease in the concentration of recombination centers. This may be responsible for the longer lifetimes in the  $n$ -type film sample studied here and for the lack of the contribution of the Shockley–Read recombination to the recombination processes.

#### 4. CONCLUSIONS

Thus, from the temperature dependences of the photosensitivity and the lifetime of nonequilibrium charge carriers in the epitaxial MCT layers grown by different procedures, we can draw a number of conclusions. In the  $n$ -type MCT films grown by MBE, the CHCC-type Auger recombination prevails in the regions of intrinsic and extrinsic conductivity. At the same time, for the  $p$ -type MCT films grown by LPE and VPE, it is found that, in the region of the extrinsic conductivity, CHLH Auger recombination is in competition with Shockley–Read recombination. The contribution of the last-mentioned component depends on the number of recombination centers and their properties and, naturally, on the procedure and conditions of preparation of the material. Thus, the  $n$ -type MBE films in which the Auger recombination mechanism prevails in the extrinsic region contain a much lower concentration of recombination

centers and hence, are of much higher quality compared to the  $p$ -type films grown by LPE and VPE.

#### REFERENCES

1. *Optical and Infrared Detectors*, Ed. by R. J. Keyes (Springer, New York, 1977; Radio i Svyaz', Moscow, 1985), p. 104.
2. A. Rogalski, *Infrared Photon Detectors* (SPIE Optical Engineering Press, Bellingham, WA, 1995), p. 145.
3. S. M. Ryvkin, *Photoelectric Effects in Semiconductors* (Fizmatgiz, Moscow, 1963; Consultants Bureau, New York, 1964), p. 39.
4. A. V. Voitsekhovskii, Yu. A. Denisov, A. P. Kokhanenko, et al., *Fiz. Tekh. Poluprovodn.* (St. Petersburg) **31**, 774 (1997) [*Semiconductors* **31**, 655 (1997)].
5. G. Busch and U. Winkler, *Bestimmung der Charakteristischen Groben eines Halbleiters aus Elektrischen, Optischen und Magnetischen Messungen* (Zürich, 1956; Inostrannaya Literatura, Moscow, 1959).
6. N. S. Baryshev, B. L. Gel'mont, and M. I. Ibragimova, *Fiz. Tekh. Poluprovodn.* (Leningrad) **24**, 209 (1990) [*Sov. Phys. Semicond.* **24**, 127 (1990)].
7. A. R. Beattie, *J. Phys. Chem. Solids* **23**, 1049 (1962).
8. T. N. Casselman, *J. Appl. Phys.* **52**, 848 (1981).
9. W. van Roosbroeck and W. Shockley, *Phys. Rev.* **94**, 1558 (1954).
10. M. Y. Pines and O. M. Stafsudd, *Infrared Phys.* **20**, 73 (1980).
11. V. C. Lopes, W. H. Wright, and A. J. Syllaios, *J. Vac. Sci. Technol. A* **8**, 1167 (1990).
12. C. E. Jones, V. Nair, and D. L. Polla, *Appl. Phys. Lett.* **39**, 248 (1981).
13. D. Rosenfeld and G. Bahir, *IEEE Trans. Electron Devices* **39**, 1638 (1992).
14. V. L. Bonch-Bruевич and S. G. Kalashnikov, *Physics of Semiconductors* (Nauka, Moscow, 1977), p. 342 [in Russian].
15. D. E. Lacklison and P. Capper, *Semicond. Sci. Technol.* **2**, 33 (1987).
16. O. L. Doyle, J. A. Mroczkowski, and J. F. Shanley, *J. Vac. Sci. Technol. A* **3**, 259 (1985).

Translated by É. Smorgonskaya